JMB
Journal of Microbiology and Biotechnology

Online ISSN : 1738-8872
Pimt ISSN : 1017-7825

JMB Papers in Press. First Published online Jul 31, 2018
DOI: 10.4014/jmb.1805.04058

Manuscript Number: JMB18-04058

Title: Stereoselective bioreduction of ethyl 3-oxo-3-(2-thienyl) propanoateusing theshort-chain dehydrogenase/reductaseChKRED12

Article Type: Research article

Keywords: Bioreduction, 3-oxoacyl-acyl-carrier-protein reductase, Short chain dehydrogenase, Duloxetine

Stereoselective bioreduction of ethyl 3-oxo-3-(2-thienyl) propanoate using the short-chain dehydrogenase/reductase *Ch*KRED12

Zhi-Qiang Ren [a, b, c]*, Yan Liu [a, c], Xiao-Qiong Pei [a, c], Zhong-Liu Wu [a, c] *

[a] Key Laboratory of Environmental and Applied Microbiology, Chengdu Institute of Biology, Chinese Academy of Sciences, Chengdu 610041, China

[b] School of Bioengineering, Sichuan University of Science & Engineering, Zigong 643000, China

[c] Environmental Microbiology Key Laboratory of Sichuan Province, Chengdu 610041, China

*Address correspondence to:

Dr. Zhi-Qiang Ren

School of Bioengineering, Sichuan University of Science & Engineering

180 Xueyuan Road,

Zigong, Sichuan 643000

P.R.China

Telephone: 86-813-5506666

Fax: 86-813-5506666

E-mail: zhiqren@foxmail.com

Prof. Zhong-Liu Wu

Chengdu Institute of Biology, Chinese Academy of Sciences

9 South Renmin Road, 4th Section

Chengdu, Sichuan 610041

P.R.China

Telephone: 86-28-82890434

Fax: 86-28-82890434

E-mail: wuzhl@cib.ac.cn

Abstract

Ethyl (*S*)-3-hydroxy-3-(2-thienyl) propanoate ((*S*)-HEES) acts as a key chiral intermediate for the blockbuster antidepressant drug duloxetine, which can be achieved via the stereoselective bioreduction of ethyl 3-oxo-3-(2-thienyl) propanoate (KEES) that contains a 3-oxoacyl structure. The sequences of the short-chain dehydrogenase/reductases from *Chryseobacterium* sp. CA49 were analyzed, and the putative 3-oxoacyl-acyl-carrier-protein reductase, *Ch*KRED12, was able to stereoselectively catalyze the NADPH-dependent reduction to produce (*S*)-HEES. The reductase activity of *Ch*KRED12 towards other substrates with 3-oxoacyl structure were confirmed with excellent stereoselectivity (>99% ee) in most cases. When coupled with a cofactor recycling system using glucose dehydrogenase, the *Ch*KRED12 was able to catalyze the complete conversion of 100 g/L KEES within 12 h, yielding the enantiopure product with >99% ee, showing a remarkable potential to produce (*S*)-HEES.

Keywords: Bioreduction; 3-oxoacyl-acyl-carrier-protein reductase; Short-chain dehydrogenase; Duloxetine

1. Introduction

Chiral compounds are very useful intermediates for the synthesis of numerous pharmaceuticals, agricultural chemicals, and specialty materials [1-5]. Among them, ethyl (*S*)-3-hydroxy-3-(2-thienyl) propanoate ((*S*)-HEES) is a useful chiral building block which is used in the synthesis of duloxetine [6-8] ((*S*)-(+)-*N*-methyl-3-(1-naphthyloxy) -3-(2-thienyl) propylamine) which is a blockbuster antidepressant drug [9-11]. (*S*)-HEES is produced *via* the asymmetric reduction of ethyl 3-oxo-3-(2-thienyl) propanoate (KEES). In recent years, the enzymatic asymmetric reduction of prochiral ketones for the preparation of optically active alcohols has gained attention [5, 12-14]. The optically pure (*S*)-HEES can be prepared by biocatalytic reductions. However, the substrate concentration applied is limited with a typical loading of 10 g/L because at higher loadings often lead to the feedback inhibition [6, 8]. Therefore, it would be necessary to search for a biocatalyst with excellent enantioselectivity and high substrate tolerance for efficient synthesis of (*S*)-HEES.

3-oxoacyl-(acyl carrier protein) reductase (3-oxoacyl-ACP reductase, EC 1.1.1.100) is a short-chain dehydrogenase/reductase that catalyzes the pyridine nucleotide-dependent reversible reduction of a 3-oxoacyl form of ACP to its hydroxyl product (Fig.1) as the first reductive step in *de novo* fatty acid biosynthesis[15, 16]. The 3-oxoacyl-ACP reductase can also catalyze the reduction of the β-keto group of unsaturated acyl chain during the biosynthesis of unsaturated fatty acid in *E. coli* [17]. The stereoselectivity of dehydrogenases/reductases can be predicted by the Prelog rule [18]; this rule indicates that an enzyme has a large and a small pocket that form the active site in which the substrate binds and controls the stereoselectivity of the product based on the geometry of the substrate and coenzyme NAD(P)H. In 3-oxoacyl-ACP reductase, the hydride ion (H^-) of NADPH is transferred from the *si*-face of ketones (3-oxoacyl-ACP) and yield *anti*-Prolog chiral alcohols ((*R*)-3-hydroxyacyl-ACP). This type of enzyme is required for the pharmaceutical industry [19, 20]. The target substrate (KEES) contains 3-oxoacyl structure (Fig. 1), it is expected to be reduced by 3-oxoacyl-ACP reductase. Using the Prelog rule to predict the steroselectivity of 3-oxoacyl-ACP reductase toward some 3-oxoacyl ester substrates, it will be transformed to (*S*)-HEES that is anti-Prelog chiral alcohol (Fig. 1).

In a previous study, we discovered 27 microbial short-chain dehydrogenase /reductases from the genome of *Chryseobacterium* sp. CA49 and expressed them in *E.*

coli [21]. Because the target substrate KEES contains a 3-oxoacyl structure (Fig. 1), the sequences of these SDRs were then analyzed to seek the reductase that had a high sequence identity with 3-oxoacyl-ACP reductase and identified *Ch*KRED12 to be an excellent catalyst to produce (*S*)-HEES with excellent enantioselectivity (>99% ee). A substrate concentration of up to 100 g/L was completely reduced with no product inhibition observed.

2. Materials and Methods

2.1 General

Substrates **2a-7a** (Table 1) were purchased from Alfa-Aesar (Tianjin, China). Substrate **1a** (Table 1) was synthesized from 2-acetylthiophene following established methods [22, 23]. The racemic alcohols were prepared by reducing the ketones with sodium borohydride [23, 24]. NADH, NADPH, $NADP^+$, isopropyl β-D-1-thiogalactopyranoside (IPTG), and glucose dehydrogenase (GDH) were purchased from Sigma (St. Louis, USA). All other reagents were obtained from general commercial suppliers and used without further purification.

2.2 Expression and purification of ChKRED12 in Escherichia coli BL21 (DE3)

The plasmid, pET-28a-*ch*KRED12, encoding *Ch*KRED12 [21] was transformed into *E. coli* BL21(DE3) (Novagen, Madison, WI, USA) competent cells and selected on Luria Bertani (LB) agar plates containing 50 μg kanamycin/mL. Single colonies were grown overnight at 37 °C in LB medium containing 50 μg kanamycin/mL. Then, 2 mL of the culture was transferred into 200 mL TB medium containing 50 μg kanamycin/mL for protein expression. When OD_{600} of the culture reached 0.8, IPTG was added to a final concentration of 1.0 mM and the cultivation was continued at 30 °C for 5 h. After harvest by centrifugation, Cells were washed twice using 20 mM sodium phosphate buffer (pH 8.0), and resuspended in buffer A (20 mM sodium phosphate buffer, 500 mM NaCl and 10 mM imidazole, pH 8.0).

After disruption with a homogenizer (Nano, ATS-AH100B, ATS Engineering Inc., Canada), the cell debris was removed by centrifugation at 2×10^4 g for 25 min at 4 °C. The resulting supernatant can be directly used as crude enzyme extracts or lyophilized to provide a dry powder of the crude enzyme. For purification, it was loaded onto Ni^{2+}-nitrilotriacetic acid columns (Bio-Rad) pre-equilibrated with buffer A. Then, the

enzyme was eluted with buffer A containing a gradient of imidazole ranging from 10 to 500 mM at a flow rate of 1 mL/min. The fractions containing the target protein were collected and dialyzed against 20 mM potassium phosphate buffer (pH 7.0). Purified enzymes were analyzed by SDS-PAGE and used for enzymatic assays. The molecular mass of the reductase was determined by elution on a Sephacryl S-200 column (1.6×90 cm) calibrated with molecular mass standards (Sigma). Protein estimations were done with a commercial BCA Protein Assay kit with bovine serum albumin as a standard (Tiangen, Beijing, China). The purified enzyme solution and lyophilized powder were stored at −80°C.

2.3 Measurement of enzyme activity

All reactions were performed in triplicate. The reaction mixture comprised 100 mM potassium phosphate buffer (pH 7.0), 10 mM NADPH and 10 mM substrate in a total volume of 1.0 ml. The reaction was carried out at 30 °C, and terminated by extraction with 1.0 ml ethyl acetate after 10 min. The resulting organic phase was subjected to gas chromatographic (GC) analysis to determine the conversion rate and ee value. One unit of the enzyme activity was defined as the amount of enzyme that catalyzes the production of 1μmol (*S*)-3-Hydroxy-3-(2-thienyl) propanoate per minute.

To determine the pH optimum, standard assay method was applied except that different buffers were used for different pH ranges, which included sodium citrate (pH 5.0-6.0), potassium phosphate (pH 6.0-8.0), Tris-HCl (pH 7.0-9.0) and sodium carbonate (pH 9.0-10.0). The optimum temperature for *Ch*KRED12 was determined at various temperatures ranging from 10 to 50 °C for 10 min. To investigate the thermostability of *Ch*KRED12, the enzyme (1 mg/ml) was incubated at 35, 40, or 45 °C, withdrawn at intervals, cooled in ice, and the residual activity was assayed following the standard assay method.

The steady-state kinetic parameters toward the substrate **1a** were investigated using standard assay method except varied substrate concentrations ranging from 0.25 to 50 mM for 5 min. The kinetic parameters toward cofactors were investigated in the presence of 10 mM **1a** for 2 min at varied cofactor concentrations ranging from 0.1 to 10 mM for NAD^+, and 1 to 200 μM for $NADP^+$, respectively, and glucose dehydrogenase was employed for coenzyme regeneration cycle (glucose dehydrogenase 10 U/ml, glucose 100 mM). Data were fitted to the Michaelis-Menten

equation using Graph-Pad Prism v5.0 (GraphPad Software, San Diego, CA, USA) to generate estimates of K_m and k_{cat} values.

2.4 Preparative-scale bioreduction

The reaction was carried out at 30 °C in 50 ml potassium phosphate buffer (100 mM, pH 8.0) containing 0.2 mM $NADP^+$, 12% (w/v)glucose, GDH (10 U/ml), crude enzyme extract or lyophilized powder of the crude enzyme (4 mg/ml, 8.4 U/mg) and the substrate concentration was 25-100 g/l. The pH of the reaction mixture was monitored and maintained at 7.0-8.0 by the addition of NaOH (1 M). To monitor the time-course of the biotransformation, samples were taken at intervals for analysis. The reaction was terminated by extraction with ethyl acetate, then the combined organic extracts were dried with anhydrous sodium sulfate, concentrated under reduced pressure and purified using silica gel column chromatography eluted with petroleum ether/ethyl acetate (10:1, v/v). The products were identified by 1H NMR analysis. The absolute configuration of the product was determined by comparing the optical rotation with the literature data.

2.5 Biotransformation of various ketones and product analysis

Standard reaction conditions were followed to convert 10 mM substrates in the presence of a coenzyme regeneration cycle (glucose dehydrogenase 10 U/mL, glucose 100 mM). The purified enzyme was applied at a concentration of 1 U/mL. After 1 h incubation at 30 °C, the reaction was terminated by extraction with ethyl acetate. The organic phase was dried with anhydrous sodium sulfate, concentrated under reduced pressure, and analyzed. The ee value and conversion of the product were determined by chiral GC analysis. Chiral GC analysis was performed on a Fuli 9790 II GC system connected to a flame ionization detector using a CP-Chirasil-DEX CB column (Varian, USA). The injector and detector were set at 260 °C and 280 °C, respectively. The column temperature was set at 160 °C (**1a**, **2a**), 120 °C (**3a**) and 90 °C (**5a**). The product of **4a** was acetylated following literature method [25] and then analyzed with chiral GC.

3. Results and discussion

3.1 Sequence analysis of ChKRED12

The sequence comparisons have shown that the typical coenzyme-binding pattern for SDRs (TGXXXGXG, Gly motif, where 'X' denotes any residues) is located at the

N-terminus of the protein chain [26, 27] and Ser-Tyr-Lys triad motif involved in catalysis and substrate binding located further to the C terminus of the protein [27, 28] (Fig. 3). These results suggested that the *Ch*KRED12 belonged to a short-chain dehydrogenase/reductase (SDR) family [21]. The sequence was compared with those in GenBank by using the BLASTp program and it was shown that the *Ch*KRED12 shares maximal identities of around 90% with 3-oxoacyl-ACP reductase, such as FabG from *Chryseobacterium daeguense* (WP 027378905.1). The alignment of the *Ch*KRED12 with 3-oxoacyl-ACP reductases, the known crystal structure of protein also showed high identity (around 40%) such as BKR from *Brassica Napus* (1EDO) [16]. Only 15-30% residue identity in pairwise comparisons, the three-dimension (3D) structures of SDR are quite similar [29]. These results indicated that the *Ch*KRED12 belonged to 3-oxoacyl-ACP reductase in SDRs family [30]. 3-oxoacyl-ACP reductase catalyzes the reduction of a 3-oxoacyl form of ACP to (*R*)-3-hydroxyacyl-ACP [31]. Therefore, it is possible that the *Ch*KRED12 has the activity to convert 3-oxoacyl substrate to (*R*)-3-hydroxyacyl isomer (Fig. 1).

3.2 Protein expression and purification

SDS-PAGE analysis indicated that the *Ch*KRED12 was highly expressed in *E. coli* BL21 (DE3) cells and that most of the recombinant protein produced was in soluble form (Fig. 4). Expression in the pET28a(+) vector resulted in the protein with an N-terminal hexa-histidine tag that facilitated purification. Single-step affinity chromatography using Ni-NTA agarose yielded the homogeneous protein (Fig. 4). SDS-PAGE showed a single band around 30kDa. The molecular mass of the *Ch*KRED12 was shown to be about 120 kDa by gel-permeation chromatography on Sephacryl S-200. Since SDS-PAGE showed a single band around 30kDa, native *Ch*KRED12 appears to be a homotetramer.

3.3 Cofactor preference and catalytic activity of ChKRED12

The *Ch*KRED12 belongs to the family of SDRs that require NADH or NADPH as a cofactor [32]. We investigated the kinetic parameters of the *Ch*KRED12 towards two cofactors at varied concentrations in the presence of 10 mM substrate **1a**. The results showed that NADPH was more efficient than NADH as a cofactor for *Ch*KRED12. The K_m values were two-folds higher and the V_{max} values were five times lower when

NADH as cofactor than NADPH (Table 1). These results indicated that the *Ch*KRED12 have a much higher binding affinity and more catalytic efficiency when NADPH as a cofactor [33], which were also consistent in cofactor preference of 3-oxoacyl-ACP reductase [27]. In biological systems, enzymes that catalyze oxidative exergonic reactions almost exclusively use NAD+/H as a cofactor and reductive endergonic reactive endergonic reactions generally utilize NADP+/H as a cofactor [34]. 3-oxoacyl-ACP reductase participates in fatty acid biosynthesis and polyunsaturated fatty acid biosynthesis, and most of them are NADPH-dependent [27, 35].

Steady-state kinetics towards substrate **1a** was measured with NADPH as a coenzyme. The apparent K_m, V_{max} and k_{cat} values were 11.8±0.6 mM, 15.2±0.3 U/mg, and 7.8±0.1 s^{-1}, respectively.

3.4 Effect of pH and temperature

The pH dependence of activities of the *Ch*KRED12 was measured using purified enzymes using **1a** as the substrate at various pH values ranging from 5.0 to 9.5 (Fig. 5). In general, the enzyme displayed broad pH adaptability. Although the maximal catalytic activity was observed in phosphate buffer at pH 8.0, yet >80% of the maximal activity could be achieved over the range of pH6.0-9.0.

The temperature dependence of the *Ch*KRED12 was measured from 10 to 50 °C. The *Ch*KRED12 displayed the maximal activity at 40°C and retained 28.6% of the maximal activity at 50 °C (Fig. 6). On the other hand, the thermostability of the enzyme should be a concern if a long-time reaction was applied. According to the thermal inactivation curve (Fig. 7), the half-lives of thermal inactivation ($t_{1/2}$) of the *Ch*KRED12 were calculated to be 46, 22 and 1.8 h at 35, 40 and 45 °C, respectively.

The *Ch*KRED12 showed a broad activity pH range, but activity was quickly lost at the temperature above 40 °C. The possible reason is that 3-oxoacyl-ACP reductase has a hydrophobic cave, which contains the active site, coenzyme binding site, and substrate binding site, and the enzymatic catalytic reaction occurs here [27, 36-38]. Because of this structure, the pH value affects the activity less before the conformation of the enzyme has been changed, but this structure cannot prevent the destruction of the conformation of the enzyme by heat when the temperature is above the optimal value.

3.5 Substrate specificity and catalytic properties

Enantiomerically pure alcohols are known as the important and valuable chiral synthons for the production of pharmaceutical and fine chemicals [39-41]. To investigate the substrate specificity of *Ch*KRED12, some substrates (Table 2, **1a**-**7a**, 10 mM) were tested. The biocatalyst reduced the substrates that contain a 3-oxoacyl structure (**1a**-**4a**) very effectively, the relative activity of over 80% were achieved for each substrate. Excellent enantioselectivity of *Ch*KRED12 was observed for **1a**, **2a**, **3a,** and **5a**, resulting in chiral alcohols of over 99%. The presence of strongly electron-withdrawing chlorine (**4a**) enhanced the catalytic efficiency and decreases stereoselectivity. In addition, *Ch*KRED12 has a higher catalytic activity for 2-oxoacyl structure substrate (**5a**) than 3-oxoacyl structure substrates (**3a**). For 2-Acetyl thiophene (**6a**) and acetophenone (**7a**) that only do not contain 3-oxoacyl structure compared with **1a** and **2a**, respectively, *Ch*KRED12 shows very low relative activity, this result suggested that 3-oxoacyl structure has a role to promote the conversion efficiency.

3.6 Preparative-scale biotransformation

The preparative-scale biotransformation was performed with the substrate **1a** in the presence of the GDH-catalyzed cofactor recycling system, using the crude enzyme that prepared from the cell extract of recombinant *E. coli*. Because the recycling system would result in the accumulation of stoichiometric gluconic acid, the pH of the reaction mixture was continuously monitored and maintained at 7.0-8.0 by the addition of 1 M NaOH. The substrate apparently did not result in inhibition at the tested substrate concentrations (125-500 mM) (Fig. 8). Complete conversion could be achieved within 2, 5, and 12 h at a concentration of substrate 25, 50, 100 g/L, respectively. Notably, there was no substrate inhibition observed. The reaction was terminated by extraction with ethyl acetate, and the combined organic extracts were dried with anhydrous sodium sulfate, concentrated under reduced pressure, and purified with column chromatography to yield (*S*)-Ethyl-3-hydroxy-3-(thiophen-2-yl) propanoate as a yellow oil (92% yield, >99% ee). 1H NMR (600 MHz, CDCl3): δ1.29 (t, 3H, J = 7.8 Hz,CH3), 2.61 (dd, 1H, J = 6.0 Hz, J = 4.8 Hz, CH2), 2.86 (dd, 1H, J = 6.0 Hz, J = 4.8 Hz, CH2), 4.12 (q, 2H, J = 6.0 Hz, CH2), 5.14 (t, 1H, J = 6.0 Hz, CHOH), 6.95 (m, 2H, Ar-H), 7.23 (m, 1H, Ar-H). (lit. [42] D25= −17.2 (c = 1.0, CHCl3) for 99%ee, (*S*)).

The reaction afforded much higher substrate tolerance than previously reported bioreduction of duloxetine precursors [6-8, 43]. For the same substrate, the previous

study used KEES reductase, which yielded compromised stereoselectivity when substrate concentration exceeded than to g/L [8]. To the best of our knowledge, the *Ch*KRED12 reported here is the best biocatalyst producing enantiopure 3-hydroxy-3-(2-thienyl) propanoate. The high-level production system for this enzyme established in this study might prove useful in the practical applications of this enzyme as a biocatalyst in the future.

4. Conclusion

This study aimed to search for a biocatalyst with excellent enantioselectivity and high substrate tolerance for KEES that contain a 3-oxoacyl structure. This type of substrate is expected to stereoselectively reduce by 3-oxoacyl-ACP reductase. The ketone reductase *Ch*KRED12 had a high sequence identity with 3-oxoacyl-ACP reductase, indicating that the *Ch*KRED12 belonged to 3-oxoacyl-ACP reductase in SDRs family and could convert 3-oxoacyl substrate to (*R*)-3-hydroxyacyl isomer. Further study showed that the *Ch*KRED12 had catalytic activities towards some 3-oxoacyl structure substrates with excellent *anti*-Prolog stereoselectivity. This reductase was successfully applied to catalyze the bioreduction of KEES to (*S*)-HEES with >99% ee value and without product inhibition, the complete conversion could be achieved within 2, 5 and 12 h at a concentration of substrate 25, 50, 100 g/L, respectively. These results demonstrated that the *Ch*KRED12 is a very promising biocatalyst to produce Ethyl (*S*)-3-hydroxy-3-(2-thienyl) propanoate (HEES) and it is expected to screen the biocatalysts based on the comparison the specificities of the enzyme with the substrate structure.

Author contributions

Zhi-Qiang Ren, Yan Liu, Xiao-Qiong Pei designed and performed the experiments. Zhi-Qiang Ren and Zhong-Liu Wu analyzed the data and wrote the manuscript.

Conflict of interest

The authors declare that they have no conflicts of interest.

Ethical approval

This article does not contain any studies with human participants or animals performed by any of the authors.

Acknowledgments

This work was supported by the National Natural Science Foundation of China (21372216 and 21572220) (to ZLW), the Key Laboratory of Environmental and Applied Microbiology (KLCAS-2015-01) (to ZQR), and the Sichuan University of Science & Engineering (2015RC45) (to ZQR).

References

1. Balke K, Kadow M, Mallin H, Sass S, Bornscheuer UT. 2012. Discovery, application and protein engineering of Baeyer-Villiger monooxygenases for organic synthesis. *Organic & biomolecular chemistry.* **10:** 6249-6265.
2. Bornscheuer UT, Huisman GW, Kazlauskas RJ, Lutz S, Moore JC, Robins K. 2012. Engineering the third wave of biocatalysis. *Nature.* **485:** 185-194.
3. Deshpande PP, Nanduri VB, Pullockaran A, Christie H, Mueller RH, Patel RN. 2008. Microbial hydroxylation of o-bromophenylacetic acid: synthesis of 4-substituted-2, 3-dihydrobenzofurans. *Journal of industrial microbiology & biotechnology.* **35:** 901-906.
4. Hollmann F, Arends IW, Holtmann D. 2011. Enzymatic reductions for the chemist. *Green Chemistry.* **13:** 2285-2314.
5. Ni Y, Xu J-H. 2012. Biocatalytic ketone reduction: a green and efficient access to enantiopure alcohols. *Biotechnology advances.* **30:** 1279-1288.
6. Ren Z-Q, Liu Y, Pei X-Q, Wang H-B, Wu Z-L. 2015. Bioreductive production of enantiopure (*S*)-duloxetine intermediates catalyzed with ketoreductase *Ch*KRED15. *Journal of Molecular Catalysis B: Enzymatic.* **113:** 76-81.
7. Tang C-G, Lin H, Zhang C, Liu Z-Q, Yang T, Wu Z-L. 2011. Highly enantioselective bioreduction of *N*-methyl-3-oxo-3-(thiophen-2-yl) propanamide for the production of (*S)*-duloxetine. *Biotechnology letters.* **33:** 1435-1440.
8. Wada M, Yoshizumi A, Furukawa Y, Kawabata H, Ueda M, Takagi H*, et al.* 2004. Cloning and overexpression of the *Exiguobacterium* sp. F42 gene encoding a new short chain dehydrogenase, which catalyzes the stereoselective reduction of ethyl 3-oxo-3-(2-thienyl) propanoate to ethyl (*S*)-3-hydroxy-3-(2-thienyl) propanoate. *Bioscience, biotechnology, and biochemistry.* **68:** 1481-1488.
9. Liu H, Hoff BH, Anthonsen T. 2000. Chemo-enzymatic synthesis of the antidepressant duloxetine and its enantiomer. *Chirality.* **12:** 26-29.
10. Bymaster F, Beedle E, Findlay J, Gallagher P, Krushinski J, Mitchell S*, et al.* 2003. Duloxetine (Cymbalta™), a dual inhibitor of serotonin and norepinephrine reuptake. *Bioorganic & medicinal chemistry letters.* **13:** 4477-4480.

11. Deeter J, Frazier J, Staten G, Staszak M, Weigel L. 1990. Asymmetric synthesis and absolute stereochemistry of LY248686. *Tetrahedron letters.* **31:** 7101-7104.
12. Nakamura K, Yamanaka R, Matsuda T, Harada T. 2003. Recent developments in asymmetric reduction of ketones with biocatalysts. *Tetrahedron: Asymmetry.* **14:** 2659-2681.
13. Goldberg K, Schroer K, Lütz S, Liese A. 2007. Biocatalytic ketone reduction—a powerful tool for the production of chiral alcohols—part II: whole-cell reductions. *Applied microbiology and biotechnology.* **76:** 249-255.
14. Sun T, Li B, Nie Y, Wang D, Xu Y. 2017. Enhancement of asymmetric bioreduction of *N*,N-dimethyl-3-keto-3-(2-thienyl)-1-propanamine to corresponding (*S*)-enantiomer by fusion of carbonyl reductase and glucose dehydrogenase. *Bioresources and Bioprocessing.* **4:** 21.
15. Toomey RE, Wakil SJ. 1966. Studies on the mechanism of fatty acid synthesis. XVI. Preparation and general properties of acyl-malonyl acyl carrier protein-condensing enzyme from Escherichia coli. *The Journal of biological chemistry.* **241:** 1159-1165.
16. Fisher M, Kroon JTM, Martindale W, Stuitje AR, Slabas AR, Rafferty JB. 2000. The X-ray structure of *Brassica napus* β-keto acyl carrier protein reductase and its implications for substrate binding and catalysis. *Structure.* **8:** 339-347.
17. Birge CH, Vagelos PR. 1972. Acyl carrier protein. XVI. Intermediate reactions of unsaturated fatty acid synthesis in *Escherichia coli* and studies of fab B mutants. *The Journal of biological chemistry.* **247:** 4921-4929.
18. Prelog V. 1964. Specification of the stereospecificity of some oxidoreductases by diamond lattice sections. *Pure and Applied Chemistry.* **9:** 12.
19. Huisman GW, Liang J, Krebber A. 2010. Practical chiral alcohol manufacture using ketoreductases. *Current opinion in chemical biology.* **14:** 122-129.
20. Tasnádi G, Hall M. 2013. Relevant Practical Applications of Bioreduction Processes in the Synthesis of Active Pharmaceutical Ingredients, pp. 329-374. *Synthetic Methods for Biologically Active Molecules*, Ed. Wiley-VCH Verlag GmbH & Co. KGaA,
21. Liu Y, Tang T-X, Pei X-Q, Zhang C, Wu Z-L. 2014. Identification of ketone reductase *Ch*KRED20 from the genome of *Chryseobacterium* sp. CA49 for highly efficient anti-Prelog reduction of 3, 5-bis (trifluoromethyl) acetophenone. *Journal of Molecular Catalysis B: Enzymatic.* **102:** 1-8.
22. Ratovelomanana-Vidal V, Girard C, Touati R, Tranchier J, Hassine BB, Genêt J. 2003. Enantioselective hydrogenation of β - keto esters using chiral diphosphine - ruthenium complexes: Optimization for academic and industrial purposes and synthetic applications. *Advanced Synthesis & Catalysis.* **345:** 261-274.
23. Takehara J, Qu JP, Kanno K, Kawabata H, Dekishima Y, Ueda M*, et al.* 2004. *3-Hydroxy-3-(2-Thienyl)Propionamide Compound, Process For Producing The Same, And Process For Producing 3-Amino-1-(2-Thienyl)-1-Propanol Compound Therefrom*.
24. Boulet SL, Filla SA, Gallagher PT, Hudziak KJ, Johansson AM, Karanjawala

RE, *et al.* 2004. *Propanamine derivatives as serotonin and norepinephrine reuptake inhibitors*.
25. Jung J, Park HJ, Uhm KN, Kim D, Kim HK. 2010. Asymmetric synthesis of (*S*)-ethyl-4-chloro-3-hydroxy butanoate using a Saccharomyces cerevisiae reductase: enantioselectivity and enzyme-substrate docking studies. *Biochimica et biophysica acta.* **1804:** 1841-1849.
26. Oppermann U, Filling C, Hult M, Shafqat N, Wu X, Lindh M, *et al.* 2003. Short-chain dehydrogenases/reductases (SDR): the 2002 update. *Chem Biol Interact.* **143-144:** 247-253.
27. Duax WL, Huether R, Pletnev V, Umland TC, Weeks CM. 2009. Divergent evolution of a Rossmann fold and identification of its oldest surviving ancestor. *International journal of bioinformatics research and applications.* **5:** 280-294.
28. Keller B, Volkmann A, Wilckens T, Moeller G, Adamski J. 2006. Bioinformatic identification and characterization of new members of short-chain dehydrogenase/reductase superfamily. *Molecular and cellular endocrinology.* **248:** 56-60.
29. Kallberg Y, Oppermann U, Jornvall H, Persson B. 2002. Short-chain dehydrogenase/reductase (SDR) relationships: a large family with eight clusters common to human, animal, and plant genomes. *Protein science : a publication of the Protein Society.* **11:** 636-641.
30. Rafferty JB, Simon JW, Baldock C, Artymiuk PJ, Baker PJ, Stuitje AR, *et al.* 1995. Common themes in redox chemistry emerge from the X-ray structure of oilseed rape (*Brassica napus*) enoyl acyl carrier protein reductase. *Structure.* **3:** 927-938.
31. Shimakata T, Stumpf PK. 1982. Purification and characterizations of beta-Ketoacyl-[acyl-carrier-protein] reductase, beta-hydroxyacyl-[acyl-carrier-protein] dehydrase, and enoyl-[acyl-carrier-protein] reductase from Spinacia oleracea leaves. *Archives of biochemistry and biophysics.* **218:** 77-91.
32. Kavanagh KL, Jornvall H, Persson B, Oppermann U. 2008. Medium- and short-chain dehydrogenase/reductase gene and protein families : the SDR superfamily: functional and structural diversity within a family of metabolic and regulatory enzymes. *Cellular and molecular life sciences : CMLS.* **65:** 3895-3906.
33. Kim TS, Patel SK, Selvaraj C, Jung WS, Pan CH, Kang YC, *et al.* 2016. A highly efficient sorbitol dehydrogenase from Gluconobacter oxydans G624 and improvement of its stability through immobilization. *Scientific reports.* **6:** 33438.
34. Cui D, Zhang L, Yao Z, Liu X, Lin J, Yuan YA, *et al.* 2013. Computational design of short-chain dehydrogenase Gox2181 for altered coenzyme specificity. *Journal of Biotechnology.* **167:** 386-392.
35. Sheldon PS, Kekwick RG, Smith CG, Sidebottom C, Slabas AR. 1992. 3-Oxoacyl-[ACP] reductase from oilseed rape (*Brassica napus*). *Biochimica et biophysica acta.* **1120:** 151-159.
36. Fisher M, Kroon JT, Martindale W, Stuitje AR, Slabas AR, Rafferty JB. 2000. The X-ray structure of Brassica napus beta-keto acyl carrier protein reductase

and its implications for substrate binding and catalysis. *Structure.* **8:** 339-347.
37. Ramachandran P, Jagtap SS, Patel SKS, Li J, Chan Kang Y, Lee J-K. 2016. Role of the non-conserved amino acid asparagine 285 in the glycone-binding pocket of *Neosartorya fischeri* β-glucosidase. *RSC Advances.* **6:** 48137-48144.
38. Selvaraj C, Krishnasamy G, Jagtap SS, Patel SKS, Dhiman SS, Kim T-S*, et al.* 2016. Structural insights into the binding mode of d-sorbitol with sorbitol dehydrogenase using QM-polarized ligand docking and molecular dynamics simulations. *Biochemical Engineering Journal.* **114:** 244-256.
39. Cai P, An M, Xu L, Xu S, Hao N, Li Y*, et al.* 2012. Development of a substrate-coupled biocatalytic process driven by an NADPH-dependent sorbose reductase from Candida albicans for the asymmetric reduction of ethyl 4-chloro-3-oxobutanoate. *Biotechnol Lett.* **34:** 2223-2227.
40. Wang LJ, Li CX, Ni Y, Zhang J, Liu X, Xu JH. 2011. Highly efficient synthesis of chiral alcohols with a novel NADH-dependent reductase from *Streptomyces coelicolor*. *Bioresour Technol.* **102:** 7023-7028.
41. Zhao FJ, Pei XQ, Ren ZQ, Wu ZL. 2016. Rapid asymmetric reduction of ethyl 4-chloro-3-oxobutanoate using a thermostabilized mutant of ketoreductase *Ch*KRED20. *Appl Microbiol Biotechnol.* **100:** 3567-3575.
42. Brem J, Liljeblad A, Paizs C, Toşa MI, Irimie F-D, Kanerva LT. 2011. Lipases A and B from *Candida antarctica* in the enantioselective acylation of ethyl 3-heteroaryl-3-hydroxypropanoates: aspects on the preparation and enantiopreference. *Tetrahedron: Asymmetry.* **22:** 315-322.
43. Soni P, Banerjee U. 2005. Biotransformations for the production of the chiral drug (*S*)-Duloxetine catalyzed by a novel isolate of Candida tropicalis. *Applied microbiology and biotechnology.* **67:** 771-777.

Figure Captions

Fig. 1 The chemical reaction catalyzes by 3-oxoacyl-ACP reductase and using the Prelog rule to predict the stereoselectivity of 3-oxoacyl-ACP reductase toward some 3-oxoacyl ester substrates.

Fig. 2 Transformation of KEES to HEES by *Ch*KRED12 coupled with a cofactor recycling system.

Fig. 3 Multiple sequence alignment of *Ch*KRED12 with several members of the SDR family. The alignment was performed with the program DNAMAN. *Ch*KRED12, short-chain dehydrogenase/reductase in this work (NCBI accession No. AHC30850.1); β-KACP-*BN*, β-keto acyl carrier protein reductase from *Brassica Napus* (PDB: 1EDO_A); CoA-AR-*BP*, Acetoacetyl-coA reductase from *Burkholderia Pseudomallei* 1710b (PDB: 3GK3_A); OR-*MT*, 3-oxoacyl-ACP reductase from *Mycobacterium Tuberculosis* H37Rv (PDB: 2NTN_A); ACPR-*HM*, β-ketoacyl-ACP reductase from *Haloarcula marismortui* (NCBI accession No. WP_004961317.1).

Fig. 4 SDS-PAGE analysis for expression and purification of *Ch*KRED12. SDS-PAGE was performed on a 12% gel under reduced conditions. Lane M, molecular weight markers; Lane 1, total proteins from *E.coli* cell containing pET28a (+) vector without induction; Lane 2, total proteins from *E.coli* cell containing pET28a (+) vector with addition 1mM IPTG; Lane 3, total proteins from *E.coli* cell containing pET28a (+)-*Ch*KRED12 construct without addition of IPTG; Lane 4, total proteins from *E.coli* cell containing pET28a (+)-*Ch*KRED12 construct with addition of 1mM IPTG; Lane 5, total soluble proteins from induced *E.coli* cell containing pET28a (+)-*Ch*KRED12 construct with addition of 1mM IPTG; Lane 6, purified recombinant *Ch*KRED12.

Fig. 5 Effect of reaction pH on the activity of the *Ch*KRED12. Four different buffers, including sodium citrate (●), Potassium phosphate (○), Tris-HCl (□), and sodium carbonate (▼) were applied.

Fig. 6 Effect of reaction temperature on the activity of the *Ch*KRED12.

Fig. 7 Thermal inactivation of the *Ch*KRED12. The enzymes were incubated at 35°C (▲), 40°C (●) and 45°C (■) for varied times and cooled on ice before the assay.

Fig. 8 Time courses of the bioreduction of ethyl 3-Oxo-3-(2-thienyl) propanoate (**1a**). at concentrations of 25 g/L (▼), 50 g/L (●), or 100 g/L (▲), using crude enzyme of the *Ch*KRED12 (4 mg/mL).

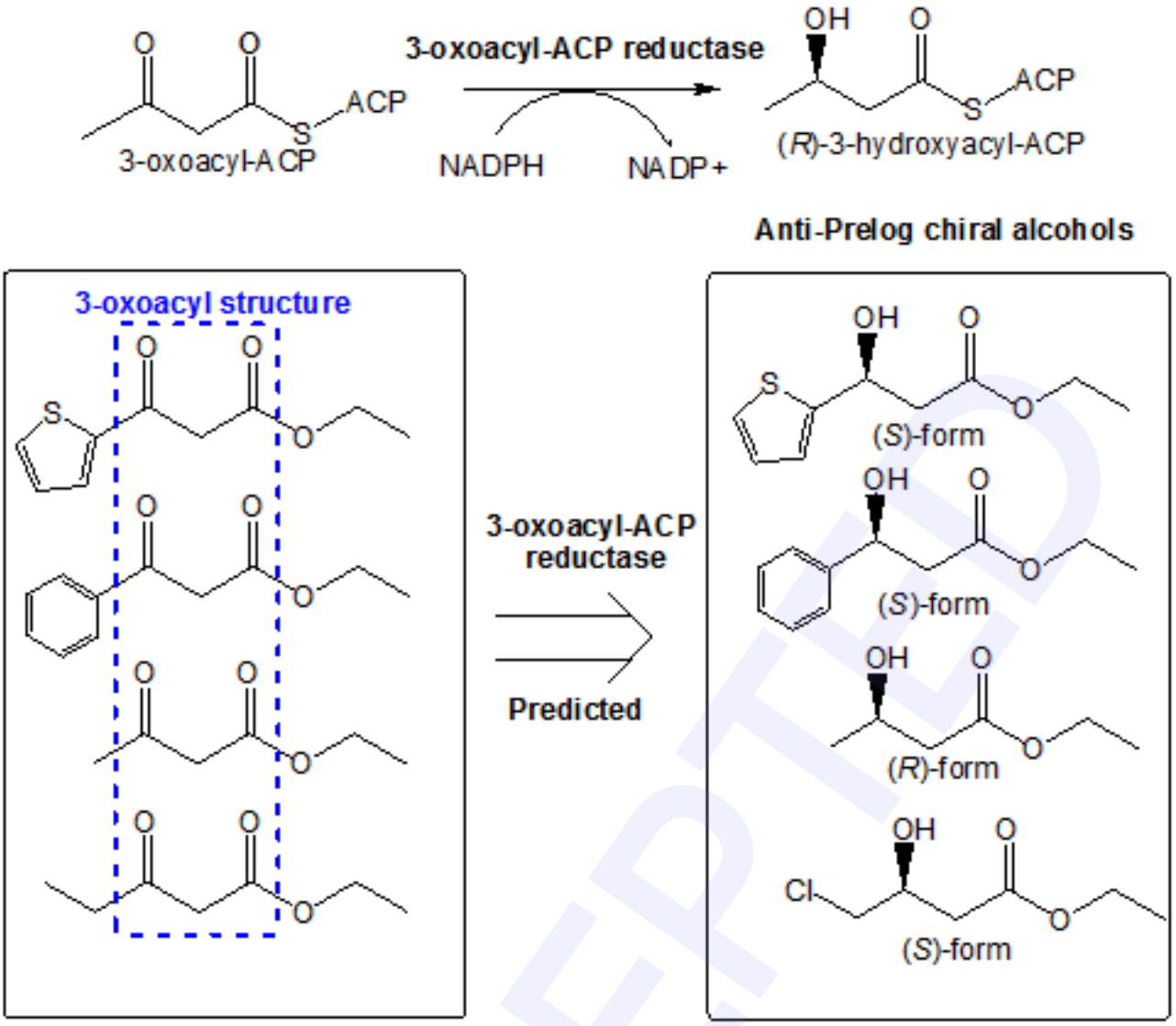

Fig. 1. The chemical reaction catalyzes by 3-oxoacyl-ACP reductase and using the Prelog rule to predict the steroselectivity of 3-oxoacyl-ACP reductase toward some 3-oxoacyl ester substrates.

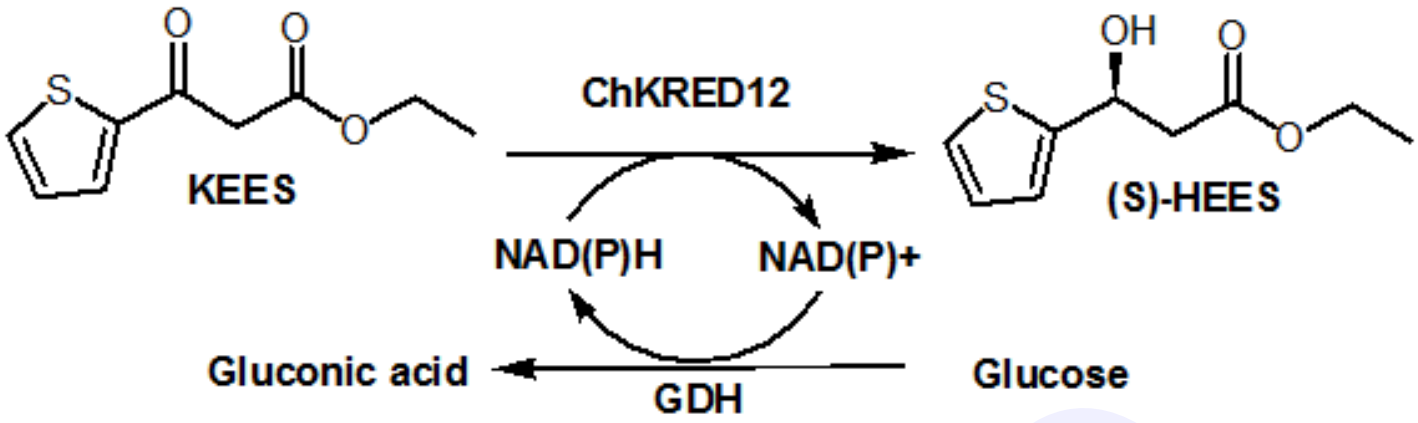

Fig. 2. Transformation of KEES to HEES by ChKRED12 coupled with a cofactor recycling system.

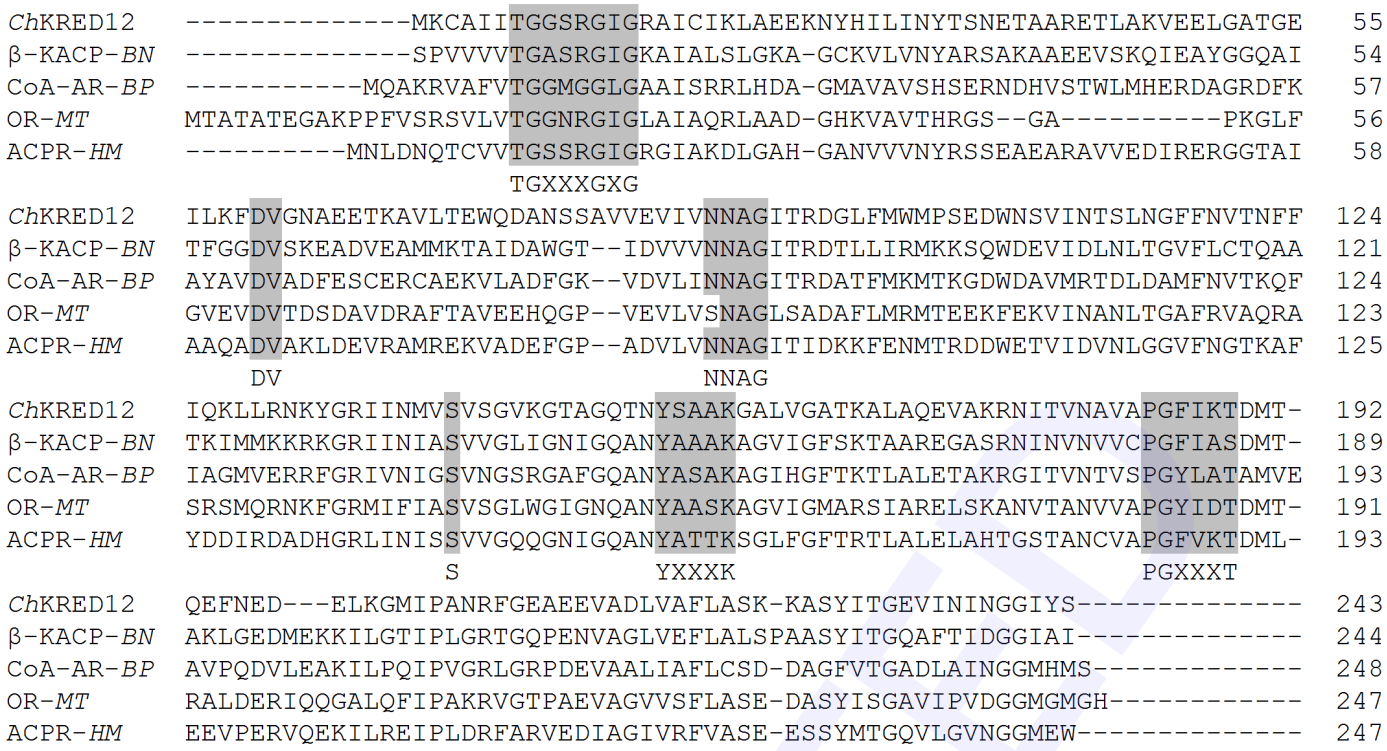

Fig. 3. Multiple sequence alignment of ChKRED12 with several members of the SDR family. The alignment was performed with the program DNAMAN. ChKRED12, short chain dehydrogenase/reductase in this work (NCBI accession No. AHC30850.1);

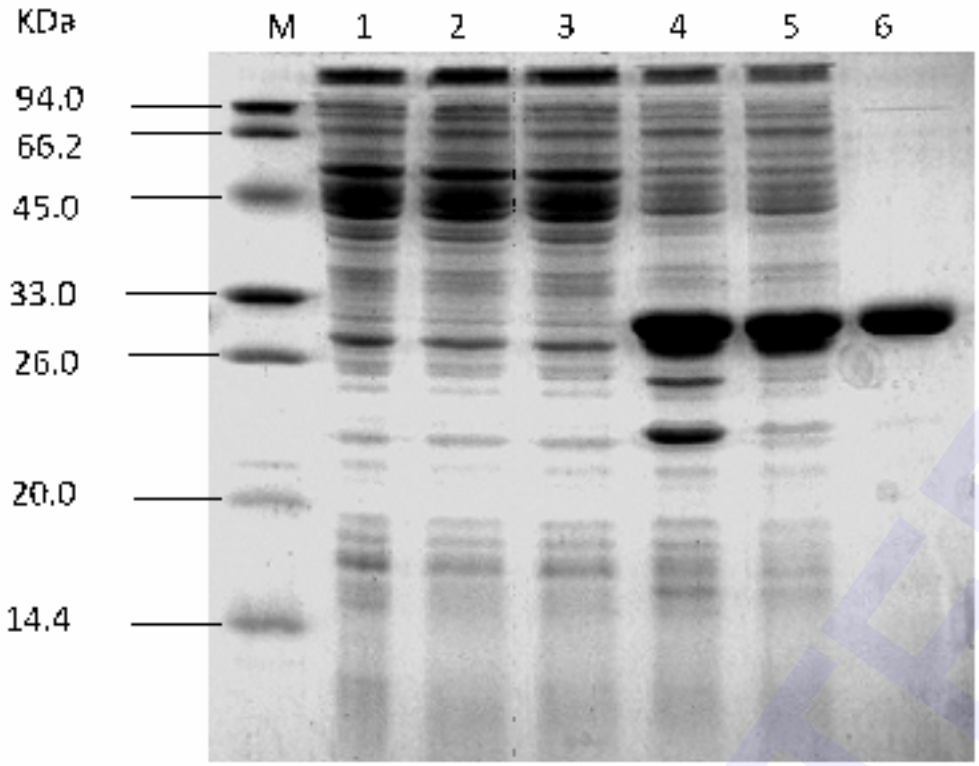

Fig. 4. SDS-PAGE analysis for expression and purification of ChKRED12. SDS-PAGE was performed on a 12% gel under reduced condition. Lane M, molecular weight markers; Lane 1, total proteins from E.coli cell containing pET28a (+) vector without induction; Lane 2, total proteins from E.coli cell containing pET28a (+) vector with addition 1mM IPTG; Lane 3, total proteins from E.coli cell containing pET28a (+)-ChKRED12 construct without addition of IPTG; Lane 4, total proteins from E.coli cell containing pET28a (+)-ChKRED12 construct with addition of 1mM IPTG; Lane 5, total soluble proteins from induced E.coli cell containing pET28a (+)-ChKRED12 construct with addition of 1mM IPTG; Lane 6, purified recombinant ChKRED12.

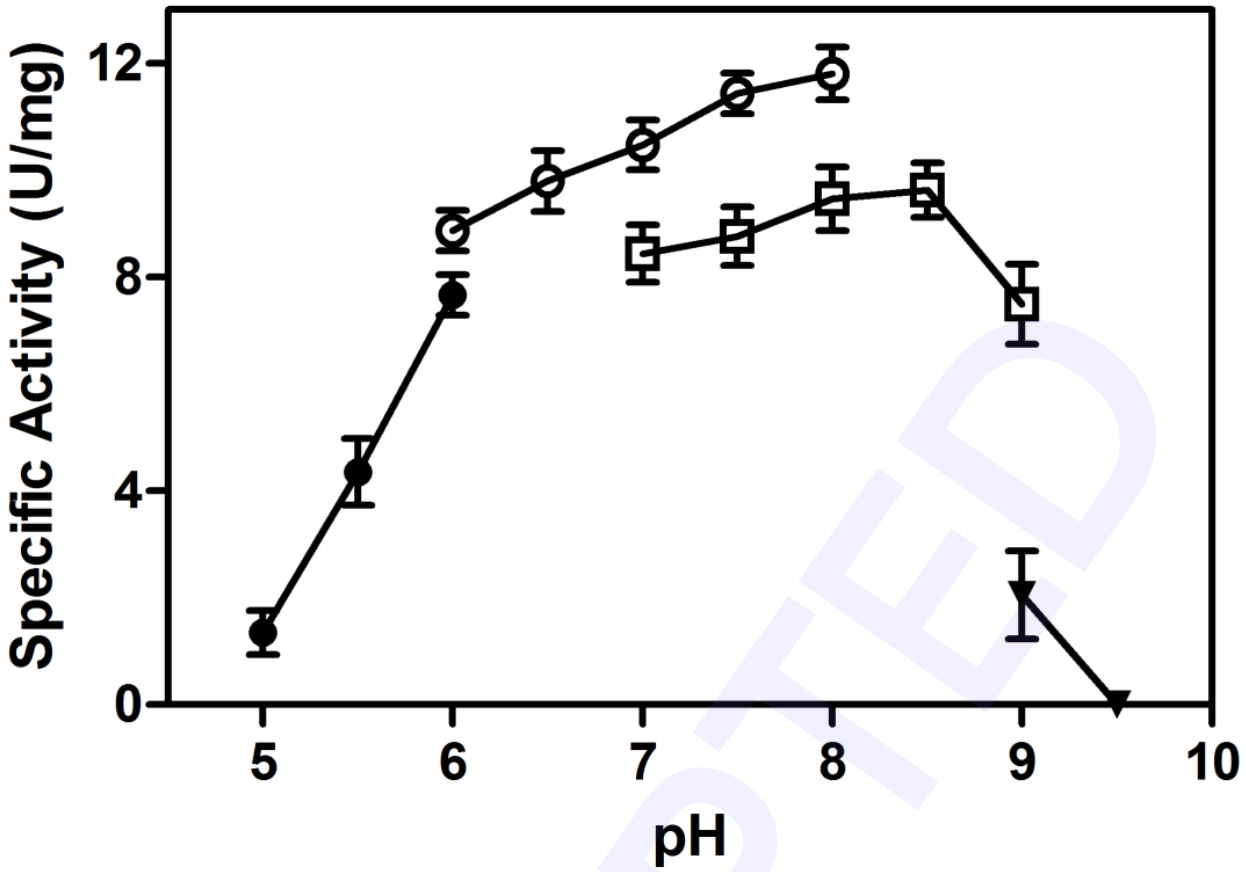

Fig. 5. Effect of reaction pH on the activity of the ChKRED12. Four different buffers, including sodium citrate (

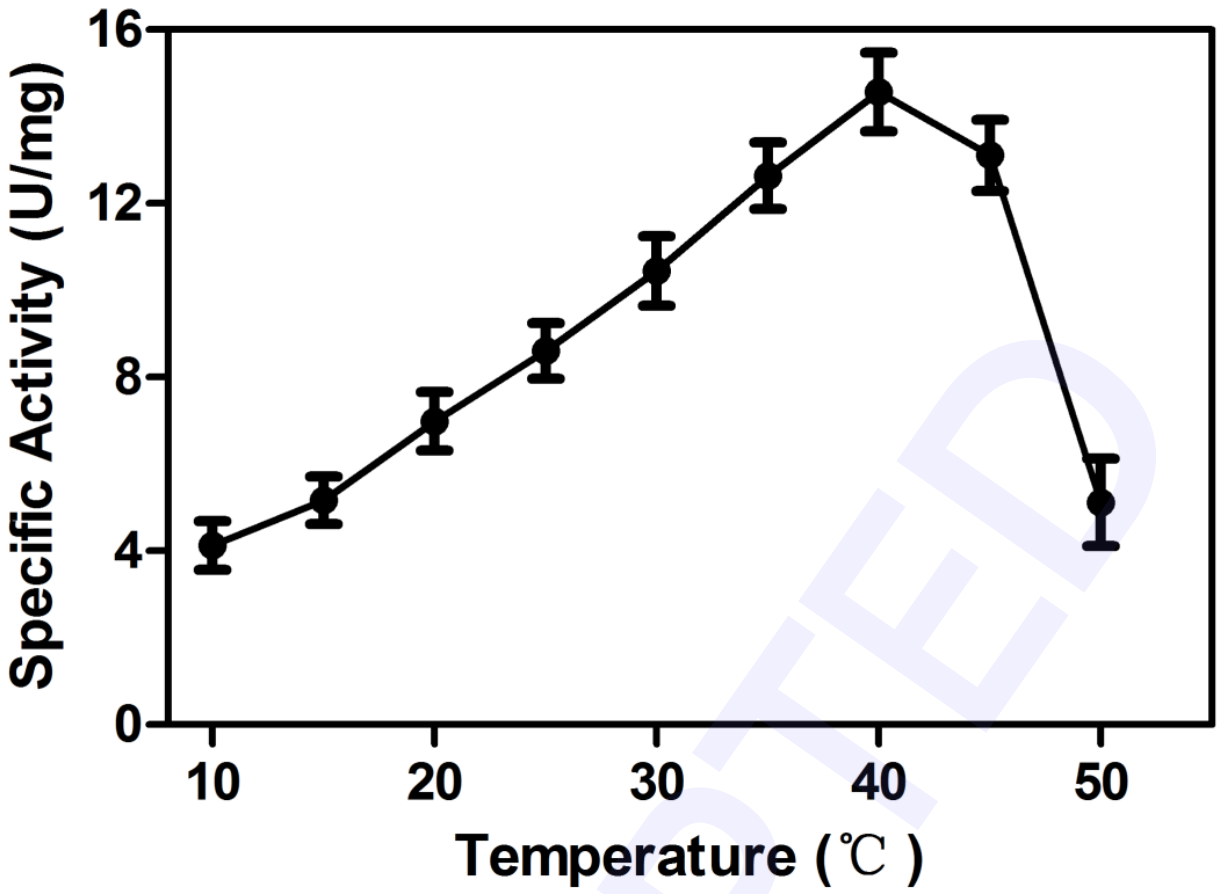

Fig. 6. Effect of reaction temperature on the activity of the ChKRED12.

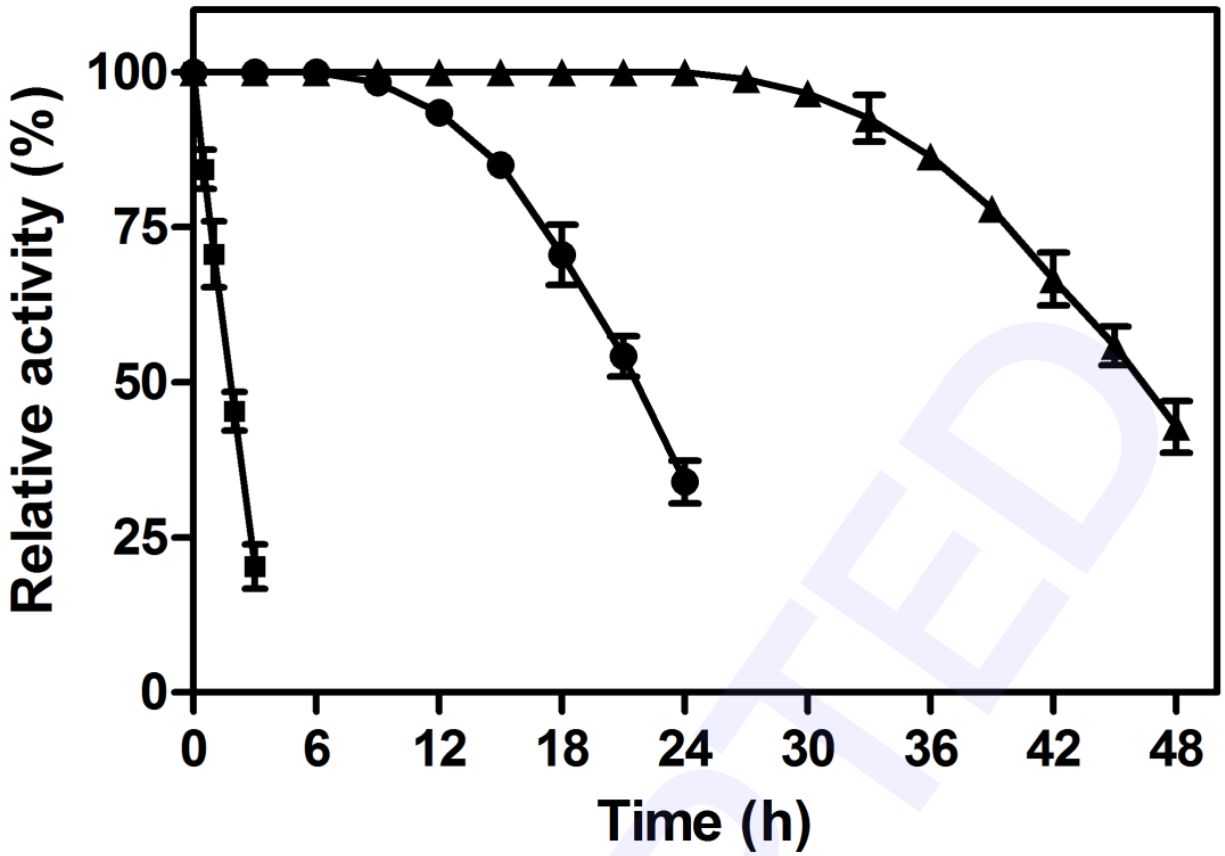

Fig. 7. Thermal inactivation of the ChKRED12. The enzymes were incubated at 35C (

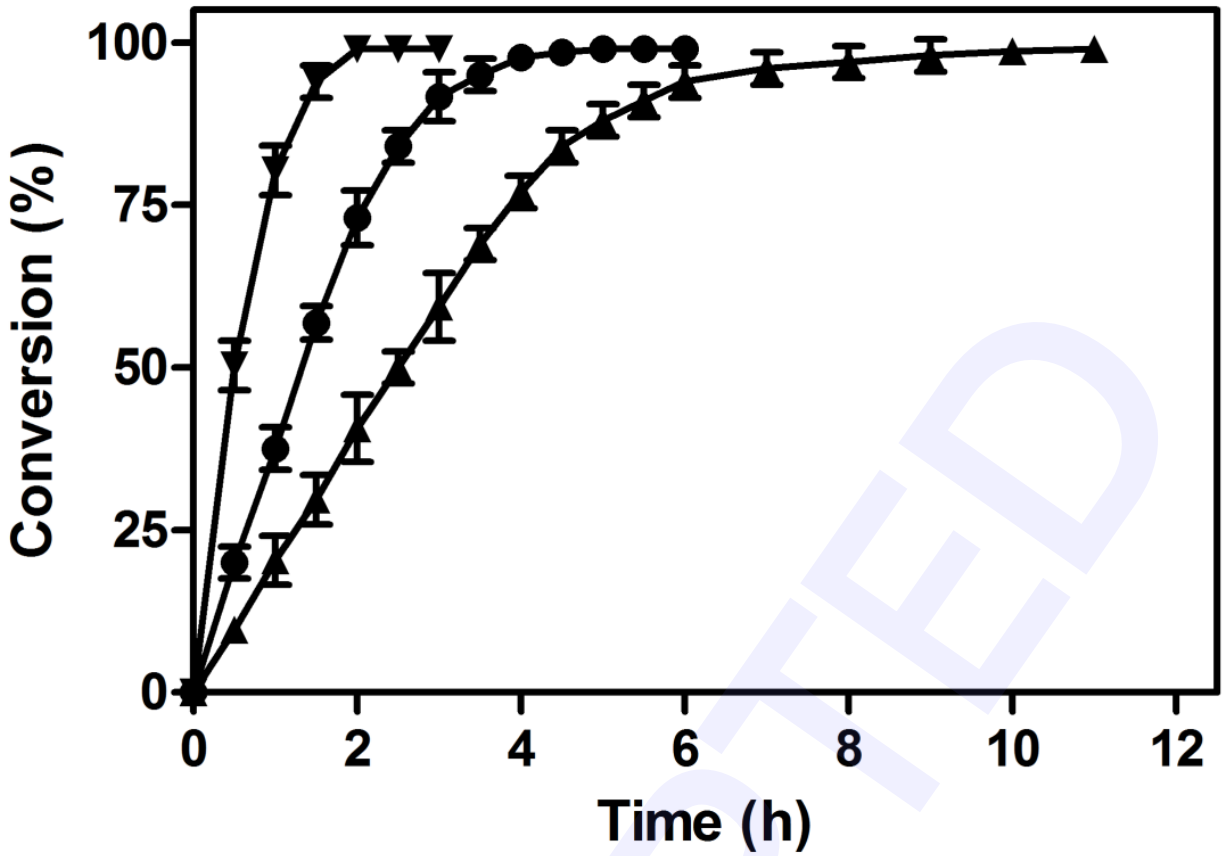

Fig. 8. Time courses of the bioreduction of ethyl 3-Oxo-3-(2-thienyl) propanoate (1a). at concentrations of 25 g/l (